Charge transfer, confinement, and ferromagnetism in $LaMnO_3/LaNiO_3$ (001) superlattices

Alex Taekyung Lee
Department of Physics, Korea Advanced Institute of Science and Technology, Daejeon 305-701, Korea

Myung Joon Han*
Department of Physics, Korea Advanced Institute of Science and Technology, Daejeon 305-701, Korea and KAIST Institute for the NanoCentury, KAIST, Daejeon 305-701, Korea

(Received 24 April 2013; published 22 July 2013)

Using first-principles density functional theory calculations, we investigated the electronic structure and magnetic properties of $(LaMnO_3)_m/(LaNiO_3)_n$ superlattices stacked along the (001) direction. The electrons are transferred from Mn to Ni, and the magnetic moments are induced at Ni sites that are paramagnetic in bulk and other types of superlattices. The size of the induced moment is linearly proportional to the amount of transferred electrons, but it is larger than the net charge transfer. The charge transfer and magnetic properties of the (m,n) superlattice can be controlled by changing the m/n ratio. Considering the ferromagnetic couplings between Mn and Ni spins and the charge-transfer characteristic, we propose the (2,1) superlattice as the largest moment superlattice. carrying $\sim 8\mu_B$ per formula unit.

DOI: 10.1103/PhysRevB.88.035126 PACS number(s): 75.70.Cn, 73.20.−r, 75.47.Lx, 71.15.Mb

I. INTRODUCTION

Recent advances in the layer-by-layer growth technique of transition metal oxide (TMO) heterostructures have created considerable research interest.[1,2] In TMO, multiple degrees of freedom (i.e., charge, spin, orbital) are coupled to each other, often creating novel material characteristics such as high-temperature superconductivity and colossal magnetoresistance.[3] By making artificial heterostructures of TMO, one can control those degrees of freedom and band structures, and therefore create or design new "correlated electron" properties. Previous TMO superlattice studies[4–8] have shown that various unexpected material phenomena can be realized at the TMO heterointerface, such as magnetism[9–11] and superconductivity.[12]

In this context, the superlattices composed of $LaNiO_3$ (LNO) and $LaMnO_3$ (LMO) are of particular interest. A recent experiment by Gibert and co-workers reported the exchange bias in LMO/LNO stacked along the (111) direction.[13] Mn-to-Ni charge transfer is expected at the LMO/LNO interface, which may cause a sizable magnetic moment in the Ni ions even if LNO is paramagnetic in bulk[3] and many other superlattices.[14–16] Importantly, however, it is quite unclear if the same mechanism is also working in the LMO/LNO superlattice stacked along (001). Although the main concern of the paper by Gibert *et al*. is the (111) structure, their data does not seem to support the same physics taking place in the (001)-stacked LMO/LNO. On the other hand, a recent extensive experimental study by Hoffman *et al*.[17] reports that the same type of charge transfer also occurs in the (001) case, and the magnetic signals were clearly observed from Ni sites. Furthermore, a recent theoretical work by Dong and Dagotto[18] suggests a different mechanism for the induced magnetic moment (M) at Ni. Their tight-binding calculations show that the induced magnetic moment in the (111) superlattice is better understood by the quantum confinement effect rather than by the charge transfer. While the effect of confinement is strongest in the (111) structure and weakest in the (001) structure, this study also raises an important question regarding the induced Ni moment in the (001) superlattice. However, due to the lack of first-principles calculations for the (001) structure, a detailed understanding of this system has not yet been achieved.

In this paper, we examine the (001) superlattice with first-principles density functional theory calculations. Our calculations of $(LMO)_m/(LNO)_n$ with several combinations of (m,n) clearly show that significant charge transfer occurs and the magnetic moments are induced at Ni sites as in the (111) case. Furthermore, the size of an induced moment is linearly proportional to the amount of charge transfer. However, the simple count of net electron transfers cannot explain the size of the moment because the up and down spins as well as the two e_g orbital degrees of freedom get involved in this process. We also found strong ferromagnetic (FM) couplings between Ni and Mn, whereas the Mn-Mn and Ni-Ni spins are antiferromagnetically aligned in some cases. As a result, superlattices with $(m,n) = (1,1)$, (1,2), and (2,1) are always FM regardless of the U value, which can have important implications for applications. Considering the amount of charge transfers and FM couplings across the interface, the (2,1) structure is proposed to have a largest moment of $\sim 8\mu_B$.

II. COMPUTATION DETAILS

For calculating $(LMO)_m(LNO)_n$ (001) superlattices ($2 \leqq m \leqq 3$, $2 \leqq n \leqq 4$), we used the projector augmented wave (PAW) potentials[19] and generalized gradient approximation (GGA) proposed by Perdew[20] for the exchange-correlation functional, as implemented in the VASP code.[21] To study the effect of electron correlation, we also used the GGA + U scheme within the rotationally invariant formalism and the double-counting formula, as first proposed by Liechtenstein *et al*.[22]

It is a long-standing problem to correctly define U and J values for the real materials. It is particularly difficult to choose the correct value of Ni-U in the LNO and the related superlattice structures. From the point of view of its atomic

character, U should not be changed much from one material to the other. However, reasonable results for LNO regarding the electronic structure can be obtained only when very small U is used. For example, Gibert *et al.* used $U = 1$ eV for Ni in their study of LMO/LNO (111) superlattices,[13] and Chakhalian *et al.* used $U = 3$ eV for their simulations of a LNO thin film.[23] For LNO/$LaAlO_3$ (LAO) superlattices, see Refs. 15,24, and 25. These values of Ni-U are quite small, especially in comparison to the Mn-U used by Gibert *et al.* and to the values adapted in other nickelate systems such as monoxide NiO.[22,26] It should also be noted that the GGA + U calculation prefers magnetic solutions and overestimates the tendency of Ni moment formation. For example, bulk LNO is predicted by GGA + U (or LDA + U) to be magnetic, which is in a sharp contrast to the reality of paramagnetism. Therefore one needs to be careful when interpreting the results of finite U calculations, especially for the bulklike Ni moment and the magnetic couplings between them.

We used four different sets of U and J for La-4f, Ni-3d, and Mn-3d states: (i) $U_{all} = J_{all} = 0$, (ii) $U_{La} = 6$ eV, $J_{La} = 0.5$ eV, $U_{Ni} = 6$ eV, $J_{Ni} = 0.5$ eV, $U_{Mn} = 5$ eV, $J_{Mn} = 0.5$ eV, (iii) $U_{La} = 3$ eV, $J_{La} = 0.5$ eV, $U_{Ni} = 3$ eV, $J_{Ni} = 0.5$ eV, $U_{Mn} = 2.5$ eV, $J_{Mn} = 0.5$ eV, and (iv) $U_{La} = 0$ eV, $J_{La} = 0$ eV, $U_{Ni} = 1$ eV, $J_{Ni} = 0$ eV, $U_{Mn} = 4$ eV, $J_{Mn} = 1$ eV. Note that the last setup for U and J is the one used by Gibert *et al.* for the (111) structure.[13] While we are mainly presenting and discussing the results from $U_{Ni} = 0$ and 3 eV, it was found that the main claims and conclusions are not changed in the other sets of parameters. The systems are predicted to be metallic by $U = 0$ and the small amount of density of states (DOS) remains at the Fermi energy also in the $U > 0$ calculations, as observed in the previous studies. By introducing the structural distortion, this small portion of DOS can be removed away from the Fermi level.[15,25]

The wave functions were expanded in plane waves with a kinetic energy cutoff of 500 eV. We used a **k**-point set generated by the $8 \times 8 \times 4$ Monkhorst-Pack mesh for the (1,1) superlattice and used equivalent **k** points for other (m,n) superlattices. Atomic positions were optimized until the residual forces were less than 0.01 eV/Å. Wigner-Seitz radii of 1.286 and 1.323 Å were used for the projection of Ni and Mn atoms, respectively, as implemented in the VASP-PAW pseudopotential. We assumed that the LMO/LNO superlattice is grown on the $SrTiO_3$ substrate by setting the in-plane lattice constant fixed at $a = b = 3.905$ Å. We used the tetragonal supercell and the optimized c-lattice parameters for each (m,n) superlattice within the FM spin configuration.

III. RESULTS AND DISCUSSION

A. Bulk and structural property

The bulk LNO is known to have a low-spin d^7 electronic configuration and to remain as a paramagnetic (PM) metal down to low temperature.[3] The local density approximation (LDA) and GGA calculation ($U = 0$) predict the correct PM ground state for the bulk phase and some other superlattice structures such as LNO/LAO and LNO/$SrTiO_3$ (STO),[14,16] while LDA + U predicts the local moment formation at the Ni site.[15,25] In our calculations, GGA + U yields the Ni moments

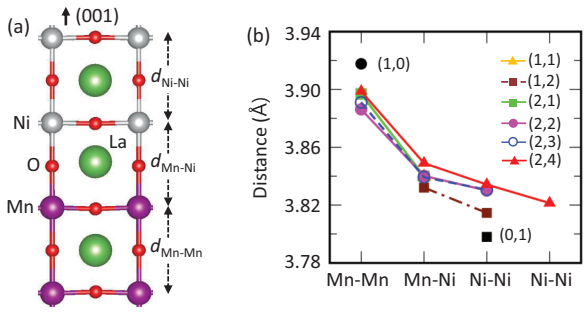

FIG. 1. (Color online) (a) Atomic structure of a $(LMO)_2/(LNO)_2$ superlattice. Gray, purple, green, and red colors stand for Ni, Mn, La, and O atoms, respectively. $d_{TM1\text{-}TM2}$ denotes the distance between the TM1 plane and TM2 plane, where TM1 and TM2 are Mn or Ni atoms. (b) The calculated $d_{Mn\text{-}Mn}$, $d_{Mn\text{-}Ni}$, and $d_{Ni\text{-}Ni}$ distances. The values for bulk LNO and LMO are indicated by $(m,n) = (0,1)$ and (1,0), respectively. Note that in (2,4), two different types of $d_{Ni\text{-}Ni}$ exist. The shorter $d_{Ni\text{-}Ni}$ corresponds to the Ni-Ni distance between the two innermost layers.

of $1.10\mu_B$ and $1.36\mu_B$ for $U = 3$ and 6 eV, respectively. In bulk LMO, Mn^{3+} has a high-spin d^4 configuration, $t_{2g}^{\uparrow 3} e_g^{\uparrow 1}$. In the GGA ($U = 0$) calculation, it is found that a small amount of $e_g^{\uparrow}$ electron is transferred to the $t_{2g}^{\downarrow}$ state due to the down-spin t_{2g} bands close to the Fermi level. The calculated magnetic moment is increased from $3.46\mu_B$ at $U = 0$ to $4.05\mu_B$ at $U = 6$ eV.

The optimized out-of-plane lattice parameter of bulk LNO and bulk LMO (with a fixed a,b lattice of STO value) are found to be $c_{LNO} = 3.798$ Å and $c_{LMO} = 3.918$ Å, respectively. In the $(LMO)_m/(LNO)_n$ superlattice, the Ni-O-Ni distance ($d_{Ni\text{-}Ni}$) and the Mn-O-Mn distance [$d_{Mn\text{-}Mn}$ in Fig. 1(a)] along the c axis are changed so that $c_{LNO} < d_{Ni\text{-}Ni}$ and $c_{LMO} > d_{Mn\text{-}Mn}$. As a result, the distances between the two transition metals (TMs) in the superlattice are always larger than c_{LNO} and smaller than c_{LMO}, as clearly shown in Fig. 1(b) for the $U = 0$ case. It is noted that the inner layer $d_{Ni\text{-}Ni}$ approaches to c_{LNO} as the thickness of the LNO layers, n, increases. We also found the same trend in the $U > 0$ results.

The bond angles of TM-O-TM in $(LMO)_m/(LNO)_n$ are generally not 180°. The in-plane angle between Mn-O-Mn (∠Mn-O-Mn) in ($m = 1$,n) superlattices is 180° since these superlattices have mirror symmetry with respect to the MnO_2 plane. On the other hand, for ($m = 2$,n) structures, ∠Mn-O-Mn decreases as n increases. Similarly, the in-plane angle between Ni-O-Ni (∠Ni-O-Ni) at the interface of ($m = 2$,n) superlattices also decreases as n increases, while ∠Ni-O-Ni ≈ 180° in (1,n) superlattices. It is noted that ∠Ni-O-Ni is increased for the bulklike Ni atoms. To see the change of the out-of-plane TM-O-TM bond angle and the possible octahedra rotations, we performed geometrical optimizations from distorted structures as starting geometries in which the atomic positions are shifted toward the in-plane oxygens (with no change in the lattice parameters). It was found that the O atoms return to their original position and the out-of-plane bond angles between Ni-O-Ni remain as 180°. Since we checked just a few cases, it does not rule out the possibility that more extensive calculations can stabilize the rotated octahedral structure, as shown in the recent literature.[25,27]

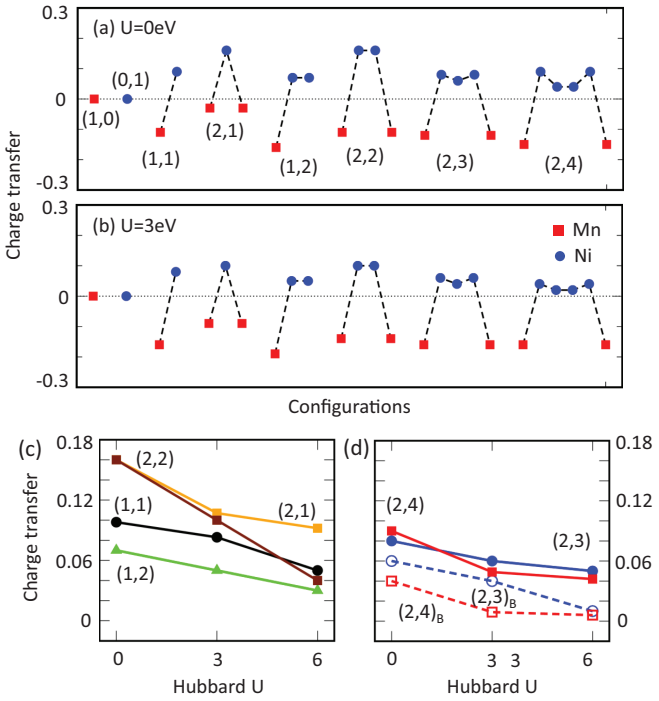

FIG. 2. (Color online) The amount of charge transfer in $(LMO)_m/(LNO)_n$ superlattices [denoted by (m,n)] calculated with (a) $U = 0$ and (b) $U = 3$ eV. Red boxes and blue circles represent the calculated charges of Mn and Ni atoms, respectively. Zero charge indicates the values from the bulk LMO and LNO. (c), (d) The amount of transferred charge to Ni as a function of U_{Ni}. $(2,3)_B$ and $(2,4)_B$ stand for the bulklike Ni atom in the (2,3) and (2,4) superlattices, respectively, while others (with no subscript) refer to the interface Ni.

B. Charge transfer and Ni magnetic moment

Figures 2(a) and 2(b) summarize the calculated result of the charge transfer between Ni and Mn for several (m,n) combinations of $(LMO)_m/(LNO)_n$, where top and bottom panels correspond to the gain and loss of electrons, respectively. The number of TM-d electrons in the bulk LNO and the bulk LMO are set to be zero as a reference point for Ni and Mn charge, respectively. The results correspond to the most stable spin configuration among all possible collinear spin orders for given (m,n) structures.[28] A clear common feature is that the electrons are transferred from Mn to Ni. Although the amount of charge transfer in the (111) case is not given in Ref. 13, we expect that the charge transfer in the (111) superlattice is larger than that in the (001) case because the (111) interface creates more Mn-O-Ni bonds than the (001) interface does. This point is also reflected in the result of the magnetic moment, which will be discussed further. The transferred electrons mostly reside at the interface Ni sites and the valence change in the bulklike (inner layer) Ni is relatively small, as clearly seen in the result of (2,3) and (2,4).

Note that, since Mn donates electrons to Ni, the amount of charge transfer and the Ni valency can be controlled by changing the superlattice composition (m,n). For a larger ratio of m/n, the induced change in the Ni valence becomes larger while that for the smaller m/n becomes smaller. By comparing the (1,1) structure with (2,1), one can find that the Ni-d occupation is larger in (2,1), where the two Mn ions can provide electrons to one Ni. The same feature is confirmed by comparing (2,2) with (2,3). As we will discuss below, the transferred electrons induce the magnetic moment at Ni, and therefore the magnetism can also be controlled by changing the superlattice compositions (m,n).[29]

The main feature regarding the charge transfer is maintained even when the on-site correlation U is turned on, as shown in Fig. 2(b). The same curve shapes are found as in the $U = 0$ results [Fig. 2(a)], indicating the same type of charge transfer. The effect of U is to reduce the amount of charge transfer onto Ni sites. $U = 6$ eV results are also found to be consistent with $U = 3$ eV [Fig. 2(b)]. The effect of correlations that reduces the Ni occupation is more clearly seen in Figs. 2(c) and 2(d), where the increase of Ni-d occupation (with respect to the bulk value) is plotted as a function of U_{Ni}. The decreasing feature is evident for all compositions of (m,n) and for both interfacial and bulklike Ni. It is noted that, in the bulklike Ni sites, the valence change caused by charge transfer is close to zero if U is large enough [see the dashed line in Fig. 2(d) at $U = 6$ eV].

For the (111) superlattices of LMO/LNO,[13] it is reported that the magnetic moment is induced at Ni, which is originally paramagnetic in bulk, and the exchange bias is manifested by this induced moment. For the (001) case, however, it is unclear if the Ni atoms are spin polarized. There is a clear controversy in the previous studies. Gibert *et al.*[13] reported that the exchange bias is not observed in the case of the (001) interface. Dong and Dagotto support this experiment by their calculations that the Ni moment is almost zero in the case of (001). On the other hand, Hoffman *et al.*[17] clearly observed the magnetic signals. Therefore, a detailed theoretical analysis is required to understand the magnetic property of the (001) structures.

Our calculations clearly show that the Ni magnetic moment is also induced in (001) superlattices. After calculating all the possible collinear spin orders for given (m,n), we present the most stable spin configurations in Figs. 3(a) and 3(b), where the top and bottom panels represent majority (up) and minority (down) spins, respectively. It is noted that the Ni ions have a nonzero spin moment even in the $U = 0$ calculations [Fig. 3(a)].

The calculated Ni moment is $\sim$0.08–0.51μ_B at $U = 0$, and enhanced up to $\sim$1.10–1.53μ_B at $U = 3$ eV. It is noted that, for the (2,2) superlattice, the calculated value of M_{Ni} is 0.47μ_B at $U = 0$, similar to the experiment $\sim$0.35μ_B.[17] As for M_{Mn}, there is a significant difference between the calculated value of 3.14μ_B and the experimental one $\sim$2μ_B (Ref. 17). Although the origin of this discrepancy is unclear, we emphasize that the calculated value is in good agreement with the Mn charge status of 4+, which is supported both by our calculation (see Fig. 2) and the x-ray absorption spectroscopy data in Ref. 17. It should be noted that for bulk LNO and other superlattices such as LNO/LAO[14,15] and LNO/STO,[16] GGA (or LDA; $U = 0$) predicts zero moment for Ni. Therefore, our result of finite Ni moments at $U = 0$ is clear evidence for the induced net moment.

It is instructive to compare the magnetic property of the (001) superlattice with (111). In both cases, the Ni magnetic moment is induced and coupled to Mn spins ferromagnetically. Also, Mn-Mn and Ni-Ni coupling is antiferromagnetic (AFM) in the (2,2) structure. The notable differences are found in the

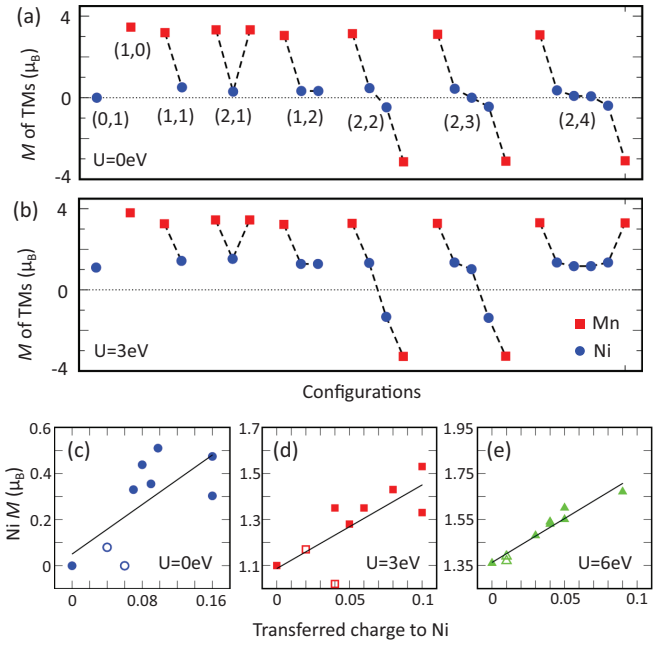

FIG. 3. (Color online) (a), (b) The calculated magnetic moments of Mn and Ni in the superlattices with (a) $U = 0$ and (b) $U = 3$ eV. Red boxes and blue circles represent the Mn and Ni values, respectively. (c)–(e) The calculated Ni magnetic moment as a function of transferred charge to Ni for (c) $U = 0$ eV, (d) $U = 3$ eV, and (e) $U = 6$ eV. Solid symbols represent the interfacial atoms, whereas open symbols represent the bulklike ones.

size of the magnetic moments. According to Gibert *et al.*,[13] $1.1 \leqslant M_{\mathrm{Ni}} \leqslant 1.4\mu_B$ for the (111) case. These values are much larger than our results for the (001) interface with $U = 0$ [see Fig. 3(a)]. To be more precise, we performed the calculations with the same U and J values as used in Ref. 13. The result clearly shows that the calculated Ni moment is always smaller in the (001) superlattice than in (111) by $\sim 0.3\mu_B$, while the Mn moment is larger in (001) by $\sim 0.3\mu_B$. Note that this trend is also consistent with the charge-transfer feature, as discussed above.

The origin of the induced moment in LMO/LNO is under debate.[13,17,18] Gibert *et al.* speculated about the charge transfer and two-dimensional confinement as a possible origin of the induced Ni moment and seem to have concluded that neither of them plays a significant role.[13] On the other hand, in an interesting recent study, Dong and Dagotto suggest that the induced moment is better understood as a result of spin-dependent quantum confinement rather than the charge transfer, especially for the case of the (111) superlattice. This confinement effect is shown to be strongest in the (111) interface and weakest in (001). Thus, further study seems necessary for the (111) case, and it is important to understand the role of confinement and charge transfer in the (001) case.

To address this point, we present the induced Ni moment as a function of the amount of electron transfer in Figs. 3(c)–3(e). A linear dependency is quite clear, especially for the nonzero U calculations, and the $U = 0$ result is not very far from the linear fit. This point suggests that the charge transfer is an important origin of the induced Ni moments in the case of the (001) superlattices. From an electronic structure point of view, the relatively larger deviation from the linear fit in the case of $U = 0$ is related to the nonmagnetic DOS of LNO. In the case of $U = 3$ or 6, the spin-down e_g band shifts upward due to the exchange splitting, and only the majority-spin bands remain around the Fermi level. Therefore, when charge transfers occur, the majority-spin bands are mainly occupied, resulting in the linear relation. At $U = 0$, on the other hand, the majority- and minority-spin bands have the same portion at the Fermi energy, and the transferred charges are distributed over both, leading to a less clear linear relation.[30] It is noted that while the size of the Ni moments is larger for $U > 0$, the moment enhancement by heterostructuring is larger in $U = 0$ because the correlation U reduces the charge transfer. It is also consistent with the picture of charge-transfer-driven moment formation.

C. Spin and orbital dependency

The number of minority-spin electrons at Mn is enhanced in the superlattice (compared to the bulk value) whereas that of Ni is mostly reduced, which is opposite to the case of majority spin. Figure 4(a) clearly shows that the sign of charge transfer is reversed in the minority-spin case [compare Fig. 4 with Fig. 2(a)]. As a result, the induced Ni moment is larger than the *net* charge transfer, and we note that this effect is largest for the (1,1) superlattice with the largest induced Ni moment.

Importantly, the occupation change of the majority spin in Ni is large, while that of the minority spin is relatively small. We note that this point is consistent with the spin-dependent quantum confinement picture suggested by Dong and Dagotto,[18] even though their analysis is best applied to the (111) interface, and the effect is relatively weak in the (001) case. In this picture, the majority-spin Ni-e_g wave function is more widely spread out while the minority-spin electron is localized. The delocalized feature of the majority-spin bands and more overlap with the neighboring up-spin Mn bands are consistent with our results that the occupation change is much larger in the majority-spin bands. For the majority spins, the Ni-d occupations decrease as U increases. In the minority-spin bands, the occupation changes are much smaller. Although the occupation changes are quite small, interestingly, the amount of occupation enhancement is found to increase as U increases, which is an opposite trend to the majority-spin case.

It is found that the largest loss and gain of electrons occur in the Mn- and Ni-$d_{3z^2-r^2}$ orbitals, respectively. Compared to the bulk value, the majority-spin Mn-$d_{3z^2-r^2}$ occupation is

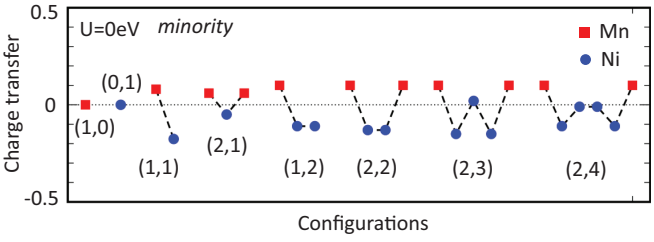

FIG. 4. (Color online) The calculated charge transfer for the minority spin ($U = 0$ eV). Red boxes and blue circles represent the Mn and Ni values, respectively. Note that the charge-transfer shape is opposite of that in Fig. 2(a).

reduced by ∼0.07–0.16 depending on (m,n) ($U = 0$ eV). The change in Mn-$d_{x^2-y^2}$ occupations is less, ∼0.02–0.11. It is due to the $d_{3z^2-r^2}$ orbital shape having more overlaps along the superlattice direction. The same feature is found in the change of Ni-e_g occupations. Ni-$d_{3z^2-r^2}$ occupations get enhanced by ∼0.12–0.18 while the Ni-$d_{x^2-y^2}$ by ∼0.06–0.10. The main features of the spin- and orbital-dependent charge occupations are maintained also in the GGA + U calculations.

D. Designing ferromagnetic superlattices

Making an FM TMO superlattice with a large magnetic moment and a high Curie temperature is an important issue for applications.[31–34] It is noted in our system that the induced Ni moment can ferromagnetically align with Mn spins as in the (111) superlattice of LMO/LNO.[13]

As summarized in Figs. 3(a) and 3(b), our calculations show that FM coupling across the interface (i.e., between Ni and Mn) is always favored energetically. That is, the interface FM spin arrangements always have less total energy than AFM ones, regardless of the other parts of spin orders and independent of U values [see Figs. 3(a) and 3(b)]. For example, the FM (1,1) superlattice has the lower total energy than the AFM one by 130 meV/$(\mathrm{LNO})_1(\mathrm{LMO})_1$ at $U = 3$ eV, which corresponds to the magnetic coupling $J_{\mathrm{Ni\text{-}Mn}} = 58$ meV with $S_{\mathrm{Mn}} = 1.6$ and $S_{\mathrm{Ni}} = 0.7$. While the Ni-Mn spins are always aligned ferromagnetically, the Mn-Mn and Ni-Ni couplings are either AFM or FM depending on U and (m,n) [see Figs. 3(a) and 3(b)].

Our result has an interesting implication in regard to the design of the magnetism of superlattices. Since the interface (Ni-Mn) coupling is always FM, the superlattice compositions of (1,1), (1,2), and (2,1) should be FM, carrying large total moments. Furthermore, the (2,1) structure is expected to have the largest moment, partly because the amount of charge transfer will be largest in this case, as we discussed already (that is, the largest m/n ratio). The calculated total moments of (1,1), (2,1), and (1,2) are $4.14\mu_B$, $7.71\mu_B$, and $4.14\mu_B$ at $U = 0$, and $5.0\mu_B$, $9.0\mu_B$, and $6.0\mu_B$ at $U = 3$ eV, respectively. It is noted that a significant amount of magnetic moment can actually be controlled by changing the (m,n) compositions.

IV. SUMMARY

Our first-principles calculations show that the magnetic moments are induced at Ni atoms in the (001)-oriented $(\mathrm{LMO})_m/(\mathrm{LNO})_n$. The induced Ni moment is governed by the electron transfer from Mn to Ni and the amount of charge transfer increases as m/n increases. Spin and orbital directions also play important roles. Our analysis, based on the FM couplings between Mn and Ni and the charge-transfer features, can provide a useful designing principle for magnetic TMO superlattices.

ACKNOWLEDGMENTS

We thank Heung-Sik Kim, Jason Hoffman, and Anand Bhattacharya for helpful discussions. This work was supported by the National Institute of Supercomputing and Networking/Korea Institute of Science and Technology Information with supercomputing resources including technical support (KSC-2013-C2-005).

*mj.han@kaist.ac.kr

[1] J. Mannhart, D. H. A. Blank, H. Y. Hwang, A. J. Millis, and J. M. Triscone, Bull. Mater. Res. Soc. **33**, 1027 (2008).
[2] H. Y. Hwang, Y. Iwasa, M. Kawasaki, B. Keimer, N. Nagaosa, and Y. Tokura, Nat. Mater. **11**, 103 (2012).
[3] M. Imada, A. Fujimori, and Y. Tokura, Rev. Mod. Phys. **70**, 1039 (1998).
[4] A. Ohtomo, D. A. Muller, J. L. Grazul, and H. Y. Hwang, Nature (London) **419**, 378 (2002).
[5] S. Okamoto and A. J. Millis, Nature (London) **428**, 630 (2004).
[6] A. Ohtomo and H. Y. Hwang, Nature (London) **427**, 423 (2004).
[7] N. Nakagawa, H. Y. Hwang, and D. A. Muller, Nat. Mater. **5**, 204 (2006).
[8] J. Chakhalian, J. W. Freeland, H.-U. Habermeier, G. Cristiani, G. Khaliullin, M. van Veenendaal, and B. Keimer, Science **318**, 1114 (2007).
[9] A. Brinkman, M. Huijben, M. van Zalk, J. Huijben, U. Zeitler, J. C. Maan, W. G. van der Wiel, G. Rijnders, D. H. A. Blank, and H. Hilgenkamp, Nat. Mater. **6**, 493 (2007).
[10] L. Li, C. Richter, J. Mannhart, and R. C. Ashoori, Nat. Phys. **7**, 762 (2011).
[11] J. A. Bert, B. Kalisky, C. Bell, M. Kim, Y. Hikita, H. Y. Hwang, and K. A. Moler, Nat. Phys. **7**, 767 (2011).
[12] N. Reyren, S. Thiel, A. D. Caviglia, L. F. Kourkoutis, G. Hammerl, C. Richter, C. W. Schneider, T. Kopp, A.-S. Rüetschi, D. Jaccard, M. Gabay, D. A. Muller, J.-M. Triscone, and J. Mannhart, Science **317**, 1196 (2007).
[13] M. Gibert, P. Zubko, R. Scherwitzl, J. Íñiguez, and J.-M. Triscone, Nat. Phys. **11**, 195 (2012).
[14] M. J. Han, C. A. Marianetti, and A. J. Millis, Phys. Rev. B. **82**, 134408 (2010).
[15] M. J. Han and M. van Veenendaal, Phys. Rev. B **85**, 195102 (2012).
[16] M. J. Han and M. van Veenendaal, arXiv:1304.1615.
[17] J. Hoffman, I. C. Tung, B. B. Nelson-Cheeseman, M. Liu, J. W. Freeland, and A. Bhattacharya, arXiv:1301.7295.
[18] S. Dong and E. Dagotto, Phys. Rev. B **87**, 195116 (2013).
[19] P. E. Blöchl, Phys. Rev. B **50**, 17953 (1994).
[20] J. P. Perdew, K. Burke, and M. Ernzerhof, Phys. Rev. Lett. **77**, 3865 (1996).
[21] G. Kresse and D. Joubert, Phys. Rev. B **59**, 1758 (1999).
[22] A. I. Liechtenstein, V. I. Anisimov, and J. Zaanen, Phys. Rev. B **52**, R5467 (1995).
[23] J. Chakhalian, J. M. Rondinelli, Jian Liu, B. A. Gray, M. Kareev, E. J. Moon, N. Prasai, J. L. Cohn, M. Varela, I. C. Tung, M. J. Bedzyk, S. G. Altendorf, F. Strigari, B. Dabrowski, L. H. Tjeng, P. J. Ryan, and J. W. Freeland, Phys. Rev. Lett. **107**, 116805 (2011).

[24]D. Puggioni, A. Filippetti, and V. Fiorentini, Phys. Rev. B **86**, 195132 (2012).

[25]A. Blanca-Romero and R. Pentcheva, Phys. Rev. B **84**, 195450 (2011).

[26]M. J. Han, T. Ozaki, and J. Yu, Phys. Rev. B **73**, 045110 (2006).

[27]H. S. Kim and M. J. Han, arXiv:1306.0713.

[28]To examine the in-plane spin structure, we calculated the total energies for the different in-plane spin configurations and found that the FM order is stabler than AFM in the (1,1) case. Based on this result, we assumed the FM in-plane order also for the larger (m,n) structures. Detailed information of the relative stability of spin configurations is presented in the Supplemental Material (Ref. 30).

[29]A small amount of electrons is also transferred onto oxygen sites. A detailed charge analysis including oxygen is presented in the Supplemental Material (Ref. 30).

[30]See Supplemental Material at http://link.aps.org/supplemental/10.1103/PhysRevB.88.035126 for magnetic stability, charge and spin analysis for oxygen sites, and a further analysis of the U dependence.

[31]U. Lüders, W. C. Sheets, A. David, W. Prellier, and R. Frésard, Phys. Rev. B **80**, 241102(R) (2009).

[32]C. Schuster, U. Lueders, U. Schwingenschloegl, and R. Fresard, arXiv:1211.2999.

[33]H. T. Dang and A. J. Millis, Phys. Rev. B **87**, 184434 (2013).

[34]H. T. Dang and A. J. Millis, Phys. Rev. B **87**, 155127 (2013).